ORIGINAL ARTICLE

Momentum removal to obtain the position-dependent diffusion constant in constrained molecular dynamics simulation

Kazushi Fujimoto[1]* | **Tetsuro Nagai**[2]* | **Tsuyoshi Yamaguchi**[3]‡

[1]Department of Materials Chemistry, Graduate School of Engineering, Nagoya University, Nagoya, Aichi 464-8603, Japan

[2]Department of Advanced Materials Science, Graduate School of Frontier Sciences, The University of Tokyo, Kashiwa, Chiba 277-8561, Japan

[3]Department of Materials Process Engineering, Graduate School of Engineering, Nagoya University, Nagoya, Aichi 464-8603, Japan

Correspondence
Tsuyoshi Yamaguchi, Department of Materials Process Engineering, Graduate School of Engineering, Nagoya University, Nagoya, Aichi 464-8603, Japan
Email: yamaguchi.tsuyoshi@material.nagoya-u.ac.jp

Funding information
Japan Society for the Promotion of Science (JSPS), KAKENHI, Grant numbers: 19K03768 and 20K05631; Ministry of Education, Culture, Sports, Science and Technology (MEXT), Program for Promoting Researches on the Supercomputer Fugaku (No. JPMXP1020200308); The Nitto Foundation.

The position-dependent diffusion coefficient along with free energy profile are important parameters needed to study mass transport in heterogeneous systems such as biological and polymer membranes, and molecular dynamics (MD) calculation is a popular tool to obtain them. Among many methodologies, the Marrink–Berendsen (MB) method is often employed to calculate the position-dependent diffusion coefficient, in which the autocorrelation function of the force on a fixed molecule is related to the friction on the molecule. However, the diffusion coefficient is shown to be affected by the period of the removal of the center-of-mass velocity, τ_{v0}, which is necessary when performing MD calculations using the Ewald method for Coulombic interaction. We have clarified theoretically in this study how this operation affects the diffusion coefficient calculated by the MB method, and the theoretical predictions are proven by MD calculations. Therefore, we succeeded in providing guidance on how to select an appropriate τ_{v0} value in estimating the position-dependent diffusion coefficient by the MB method. This guide-

Abbreviations: COM, Center of mass; FACF, Force autocorrelation function; MB, Marrink–Berendsen; MD, Molecular Dynamics; WR, Woolf–Roux.

* Equally contributing authors.

line is applicable also to the Woolf–Roux method.

KEYWORDS
Position-dependent diffusion coefficient, Marrink–Berendsen method, Woolf–Roux method, Molecular dynamics calculation

1 | INTRODUCTION

Mass transport phenomena in heterogeneous systems are important issues in various fields, and much research has been conducted in this area to date. For example, in the field of biological chemistry, understanding the permeation of drugs into viruses[1] and through membranes[2–4] at the molecular level plays an important role in appropriate rational drug design. In the field of materials sciences such as in the separation of molecules using reverse osmosis membranes[5,6] and the study of the transport process of protons, oxygen, and hydrogen in a polymer electrolyte membrane[7–9], it is important to understand the relationship between the mechanism of molecular transport and the microscopic details of the materials.

The position-dependent diffusion coefficient, along with the free energy profile, is an important physical quantity utilized in studies of the mass transport phenomena of heterogeneous systems using molecular dynamics (MD) calculations. Because of its importance, many methods[10–19] have been proposed to obtain the position-dependent diffusion coefficient. Two of us and other coworkers have also previously proposed a method for obtaining the position-dependent diffusion coefficient with high accuracy in any heterogeneous system[20].

Among the methods proposed so far, the Marrink–Berendsen (MB) method is one of the best-known methods used to calculate the position-dependent diffusion coefficient[21–26]. This method allows for straightforward calculation of the the position-dependent diffusion coefficient with existing MD calculation packages. In this method, the center of mass (COM) of the molecule is constrained to a certain position, and the diffusion coefficient can be obtained by the force autocorrelation function (FACF) of the COM of the molecule. A downside is systematic underestimation of the resultant diffusion coefficient[27,20], which can be attributed to perturbation of dynamics arising from constraints. In other words, the memory kernel of a freely moving particle may not always be well approximated by that of a constrained particle.

In this paper, we demonstrate the critical role of momentum removal in obtaining the position-dependent diffusion coefficient by methods involving position constraints, such as the MB method. In MD calculations that use the Ewald method[28,29] for calculating the long-range Coulombic interaction, the momentum of the MD system is reduced to zero with a certain time interval, τ_{v0}, to prevent the MD system from diffusing. We demonstrate that this operation affects the diffusion coefficient calculated by the MB method when constraining the diffusing molecules to absolute coordinates. In particular, the diffusion coefficient can be overestimated without the operation. In this paper, we propose a theoretical equation comparing FACFs with and without the COM momentum removal. The theoretical equation was then examined to find the diffusion coefficient of methane in water. It was also found that τ_{v0} dependence varies with the size of the system in the MD calculation. The theory we propose in this paper plays an important role in obtaining the position-dependent diffusion coefficient in three-dimensional heterogeneous systems using the MB method. The method with spring restraint on absolute values, proposed by Woolf and Roux (WR method),[12] is also discussed.

2 | THEORY

The change in FACF, $\langle \mathbf{F}(0) \cdot \mathbf{F}(t) \rangle$, with changing τ_{v0} is explained qualitatively in terms of the momentum conservation within the whole simulation cell. Suppose that a solute molecule of infinite dilution feels force from the surrounding solvent in the $+z$ direction at $t = 0$. The force between the solute and the solvent means the momentum exchange between them, and the momentum in the $-z$ direction is then transferred from the solute to the solvent. The momentum given by the solvent is further transported to the bulk solvent with time through solvent–solvent interactions. In the MD simulation cell of finite size, however, the momentum in the $-z$ direction cannot dissipate due to the momentum conservation, and the momentum is instead distributed uniformly over the whole simulation cell after sufficient time, which means the solvent flows in the $-z$ direction. The fixed solute in the solvent flow in the $-z$ direction then feels frictional force in the $-z$ direction, leading to a negative correlation between $\mathbf{F}(0)$ and $\mathbf{F}(t)$. A shift of the COM velocity of the solvent eliminates the negative correlation, and its operation frequency, $1/\tau_{v0}$, affects the strength of the negative correlation at longer time durations. The physics concepts outlined above are described quantitatively hereafter in this section using projection operator formalism.

The system under consideration is composed of a solute (X) and a finite number of solvent molecules (S), which are contained in a cell with periodic boundary conditions. The solute is fixed at a given spatial position and no other external force operates on the solvent. A shift of the COM velocity of the solvent is not performed.

The COM velocity of the solvent, $\mathbf{v}_{CM}$, is defined as follows:

$$\mathbf{v}_{CM} \equiv \frac{1}{M_S} \sum_{i \in S} m_i \mathbf{v}_i, \tag{1}$$

$$M_S \equiv \sum_{i \in S} m_i. \tag{2}$$

Here, the summations run over all the solvent molecules, and the mass and the velocity of the i-th solvent molecule are described as m_i and $\mathbf{v_i}$, respectively. The projection operator onto $\mathbf{v}_{CM}$ is defined as $\mathcal{P}$, and the projection operator to the orthogonal space is given by $\mathcal{Q} \equiv 1 - \mathcal{P}$. The definition of the projection operator, $\mathcal{P}$, is explicitly given by

$$\mathcal{P}\mathbf{A} \equiv \frac{\langle \mathbf{v}_{CM} \cdot \mathbf{A} \rangle}{\left\langle |\mathbf{v}_{CM}|^2 \right\rangle} \mathbf{v}_{CM} = \frac{M_S}{3k_B T} \langle \mathbf{v}_{CM} \cdot \mathbf{A} \rangle \mathbf{v}_{CM}, \tag{3}$$

where $\mathbf{A}$ is an arbitrary vector variable. The Boltzmann constant and the absolute temperature are denoted here as k_B and T, respectively.

An identity below holds for the time propagation operator as [30]

$$e^{i\mathcal{L}t}\mathcal{Q} = e^{i\mathcal{Q}\mathcal{L}\mathcal{Q}t} + \int_0^t d\tau e^{i\mathcal{L}(t-\tau)} \mathcal{P} i\mathcal{L} e^{i\mathcal{Q}\mathcal{L}\mathcal{Q}\tau}, \tag{4}$$

where $\mathcal{L}$ stands for the Liouvillian operator. Equation (4) is then multiplied by the force on the solute, $\mathbf{F}_X$, from the left to yield

$$\begin{aligned} e^{i\mathcal{L}t}\mathbf{F}_X \quad = \quad & e^{i\mathcal{Q}\mathcal{L}\mathcal{Q}t}\mathbf{F}_X - \frac{M_S}{3k_B T} \int_0^t d\tau \left[e^{i\mathcal{L}(t-\tau)} \mathbf{v}_{CM} \right] \\ & \times \left\langle \{ i\mathcal{L}\mathbf{v}_{CM} \} \cdot \left\{ e^{i\mathcal{Q}\mathcal{L}\mathcal{Q}\tau} \mathbf{F}_X \right\} \right\rangle. \end{aligned} \tag{5}$$

The Hermitian property of the Liouvillian operator,

$$\langle \mathbf{A} \cdot \{ i\mathcal{L}\mathbf{B} \} \rangle = - \langle \{ i\mathcal{L}\mathbf{A} \} \cdot \mathbf{B} \rangle , \tag{6}$$

is utilized in the derivation from Equations (4) to (5), where $\mathbf{A}$ and $\mathbf{B}$ stand for arbitrary vector quantities.

The momentum conservation of the whole system relates $\mathbf{F}_X$ and $\mathbf{v}_{CM}$ as

$$\mathbf{F}_X + M_S \{ i\mathcal{L}\mathbf{v}_{CM} \} = 0, \tag{7}$$

which is substituted into Eq. (5) to give

$$\begin{aligned} e^{i\mathcal{L}t}\mathbf{F}_X &= e^{iQ\mathcal{L}Qt}\mathbf{F}_X + \frac{1}{3k_BT}\int_0^t d\tau \left[e^{i\mathcal{L}(t-\tau)}\mathbf{v}_{CM} \right] \\ &\quad \times \left\langle \mathbf{F}_X \cdot \left\{ e^{iQ\mathcal{L}Q\tau}\mathbf{F}_X \right\} \right\rangle . \end{aligned} \tag{8}$$

We change the notations here as follows:

$$\mathbf{F}_X(t) \equiv e^{i\mathcal{L}t}\mathbf{F}_X, \tag{9}$$

$$\mathbf{R}_X(t) \equiv e^{iQ\mathcal{L}Qt}\mathbf{F}_X, \tag{10}$$

$$\mathbf{v}_{CM}(t) \equiv e^{i\mathcal{L}t}\mathbf{v}_{CM}, \tag{11}$$

$$\gamma(t) \equiv \frac{1}{3k_BT} \langle \mathbf{R}_X(0) \cdot \mathbf{R}_X(t) \rangle . \tag{12}$$

Equation (8) is then rewritten with these notations as

$$\mathbf{F}_X(t) = \mathbf{R}_X(t) + \int_0^t d\tau \gamma(t-\tau)\mathbf{v}_{CM}(\tau). \tag{13}$$

In Eq. (13), the total force acting on the solute at time t, $\mathbf{F}_X(t)$, is divided into the sum of random force, $\mathbf{R}_X(t)$, and the drag force by the flow of the solvent.

The statistical average of Eq. (13) after the multiplication of $\mathbf{F}_X(0) = \mathbf{R}_X(0)$ gives

$$\begin{aligned} \langle \mathbf{F}_X(0) \cdot \mathbf{F}_X(t) \rangle &= \langle \mathbf{R}_X(0) \cdot \mathbf{R}_X(t) \rangle + \int_0^t d\tau \gamma(t-\tau) \\ &\quad \times \langle \mathbf{F}_X(0) \cdot \mathbf{v}_{CM}(\tau) \rangle . \end{aligned} \tag{14}$$

The time correlation function in the integral, $\langle \mathbf{F}_X(0) \cdot \mathbf{v}_{CM}(\tau) \rangle$, is further related to FACF as

$$\langle \mathbf{F}_X(0) \cdot \mathbf{F}_X(t) \rangle + M_S \frac{d}{dt} \langle \mathbf{F}_X(0) \cdot \mathbf{v}_{CM}(t) \rangle = 0 \tag{15}$$

by virtue of Eq. (7).

The MB method is used to evaluate approximately the time correlation function of the random force acting on a freely moving solute as that of the total force on the spatially fixed one [11]. The time correlation function of the random force is then converted into the time-dependent friction coefficient through Eq. (12), and the position-dependent diffusion coefficient can then be determined. According to Eq. (14), however, the time correlation function of the

total force, $\langle \mathbf{F}_X(0) \cdot \mathbf{F}_X(t) \rangle$, contains the correlation with the drag force, in addition to the time correlation function of the random force, $\langle \mathbf{R}_X(0) \cdot \mathbf{R}_X(t) \rangle$. What we actually want to determine is the latter correlation function, and we need to somehow eliminate the second term of Eq. (14).

The time development of the random force is governed by the projected Liouvillian, $\mathcal{QLQ}$, instead of the normal one, $\mathcal{L}$. Since the dynamics of the random force are determined by that of the positions and the momenta of the solvent molecules, $\{\mathbf{r}_i, \mathbf{p}_i\}$, the effects of the replacement of the Liouvillian can be analyzed through their dynamics. The time dependence of $\mathbf{r}_i$ and $\mathbf{p}_i$ through $\mathcal{QLQ}$ is explicitly written as follows:

$$i\mathcal{QLQ}\mathbf{r}_i = \frac{1}{m_i}\mathbf{p}_i - \frac{1}{M_S}\sum_{j\in S}\mathbf{p}_j, \tag{16}$$

$$i\mathcal{QLQ}\mathbf{p}_i = \mathbf{F}_i - \frac{m_i}{M_S}\sum_{j\in S}\mathbf{F}_j, \tag{17}$$

where $\mathbf{F}_i$ stands for the force acting on the solvent molecule i. The derivation of these equations is described in Sec. S1 of Supporting Information. In Eqs. (16) and (17), the first terms of the right-hand sides give the ordinary time dependence through $\mathcal{L}$, and the second terms mean the shift of the COM velocity. Therefore, the dynamics given by the projected Liouvillian, $\mathcal{QLQ}$, corresponds to the time propagation of MD simulation in which the shift of the COM velocity is performed at *every* step, and the autocorrelation function of the force in such MD simulation can be regarded as that of $\mathbf{R}_X(t)$. It is thus expected that a smaller τ_{v0} leads to a better diffusion coefficient in the implementation of the MB method in MD simulation.

The long-time limiting behaviors of $\langle \mathbf{F}_X(0) \cdot \mathbf{F}_X(t) \rangle$ can be analyzed based on Eqs. (14) and (15). First, the integral of Eq. (15) from $t = 0$ to ∞ gives

$$\int_0^\infty dt\, \langle \mathbf{F}_X(0) \cdot \mathbf{F}_X(t) \rangle = M_S \left[\langle \mathbf{F}_X(0) \cdot \mathbf{v}_{CM}(0) \rangle - \langle \mathbf{F}_X(0) \cdot \mathbf{v}_{CM}(\infty) \rangle \right]. \tag{18}$$

The first term of the right-hand side vanishes so long as $\mathbf{F}_X$ does not depend on the velocity of the solvent explicitly. The second term is also zero because the correlation is lost after the infinite time interval. Therefore, the integral of $\langle \mathbf{F}_X(0) \cdot \mathbf{F}_X(t) \rangle$ on the left-hand side is equal to zero. It should be noted that the discussion above does not apply to an infinite-size system where M_S diverges.

The time derivative of Eq. (14), combined with Eq. (15) yields

$$\frac{d}{dt}\langle \mathbf{F}_X(0) \cdot \mathbf{F}_X(t) \rangle = \frac{d}{dt}\langle \mathbf{R}_X(0) \cdot \mathbf{R}_X(t) \rangle - \frac{1}{M_S}\int_0^t d\tau \gamma(t-\tau) \langle \mathbf{F}_X(0) \cdot \mathbf{F}_X(\tau) \rangle. \tag{19}$$

Provided that the relaxation of $\gamma(t)$ is relatively fast, Eq. (19) can be approximated in the time scale longer than the relaxation time of $\gamma(t)$ as

$$\frac{d}{dt}\langle \mathbf{F}_X(0) \cdot \mathbf{F}_X(t) \rangle \simeq -\frac{1}{M_S}\left[\int_0^\infty d\tau \gamma(\tau)\right] \langle \mathbf{F}_X(0) \cdot \mathbf{F}_X(t) \rangle. \tag{20}$$

It means that $\langle \mathbf{F}_X(0) \cdot \mathbf{F}_X(t) \rangle$ decays exponentially as

$$\langle \mathbf{F}_X(0) \cdot \mathbf{F}_X(t) \rangle \propto e^{-\frac{t}{\tau_{FF}}}, \tag{21}$$

with the time constant given by

$$\tau_{FF} = \frac{M_S}{\int_0^\infty d\tau \gamma(\tau)}. \tag{22}$$

3 | METHOD

3.1 | Molecular dynamics calculation

The effect of the frequency of the shift of the COM velocity on the time correlation function was investigated by performing simulations with different τ_{v0} values. Here, τ_{v0} denotes the interval between the removals of the COM velocity during MD simulations. System-size dependence was also investigated by studying two methane solutions of different sizes. The smaller system was composed of a methane molecule and 1053 water molecules and was simulated with τ_{v0} set at 1 fs, 0.1 ps, 10 ps, and ∞. As to the larger system consisting of a methane molecule and 8424 water molecules, τ_{v0} was set at 0.1 ps, 10 ps, and ∞. Since the time step of the MD simulation was set at 1 fs as described below, the simulation with $\tau_{v0} = 1$ fs corresponds to a faithful realization of the dynamics as defined by Eqs. 16 and 17, whereby $\mathbf{R}_X(t)$ can be directly and accurately evaluated. Moreover, simulations with $\tau_{v0} = \infty$ correspond to the dynamics defined by the Liouvillian operator. These simulations enable the measurement of $\mathbf{F}_X(t)$. Hereafter, the FACF obtained by MD with τ_{v0} is denoted by $C_{\mathrm{FF}}^{\mathrm{sim}}(t;\tau_{v0}) \equiv \left\langle \mathbf{F}^{\mathrm{sim}}(t;\tau_{v0}) \cdot \mathbf{F}^{\mathrm{sim}}(0;\tau_{v0}) \right\rangle$ to explicitly express the dependence on τ_{v0}.

After routine equilibration, each of the production runs was performed in the NVT ensemble for 50 ns with a time step of 1 fs. The temperature was controlled by a Nosé–Hoover thermostat [31,32] at 300 K with a time constant of 100 fs. The effect of the thermostat on the resultant diffusion constant has been shown to be negligible in these conditions [20] for various methods, thus allowing us to get the position-dependent diffusion constant. The total force acting on the COM of the methane molecule was sampled every 1 fs. The electrostatic potential was calculated by the particle mesh Ewald method with a short-range cutoff length of 1.2 nm. The van der Waals interaction was cut off at 1.2 nm and the cutoff correction applied. All simulations were performed using GROMACS 2019 [33], which was modified to constrain the methane molecule. The water molecules were modeled by the SPC model [34] and the methane molecule was modeled by OPLS-UA [35].

3.2 | Analysis

We demonstrated numerically the satisfaction of Eq. 14 and thereby the theoretical framework described in the aforementioned section. To achieve this, we evaluated $\langle \mathbf{F}_X(0) \cdot \mathbf{F}_X(t) \rangle$ and $\langle \mathbf{R}_X(0) \cdot \mathbf{R}_X(t) \rangle$. Given these time correlation functions, the integrand on the right hand-side of Eq. 14 can be obtained via Eqs. 12 and 15. In particular, $\langle \mathbf{F}_X(0) \cdot \mathbf{v}_{CM}(\tau) \rangle$ was obtained by integrating $\langle \mathbf{F}_X(0) \cdot \mathbf{F}_X(t) \rangle$ from zero to τ (see Eq. 15). The time correlation function $\langle \mathbf{F}_X(0) \cdot \mathbf{F}_X(t) \rangle$ was evaluated as $\left\langle \mathbf{F}^{\mathrm{sim}}(t;\infty) \cdot \mathbf{F}^{\mathrm{sim}}(0;\infty) \right\rangle$ or the force autocorrelation function obtained from the trajectories with $\tau_{v0} = \infty$, as these trajectories are the realization of dynamics of the Liouvillian operator. As regards the smaller system, $\langle \mathbf{R}_X(0) \cdot \mathbf{R}_X(t) \rangle$ was calculated from the trajectory with $\tau_{v0} = 1$ fs, which is a

faithful realization of the dynamics defined by Eqs. 16 and 17. In other words, $\langle \mathbf{R}_X(0) \cdot \mathbf{R}_X(t) \rangle$ was calculated by $\left\langle \mathbf{F}^{\mathrm{sim}}(t; 1\ \mathrm{fs}) \cdot \mathbf{F}^{\mathrm{sim}}(0; 1\ \mathrm{fs}) \right\rangle$. For the larger system, $\langle \mathbf{R}_X(0) \cdot \mathbf{R}_X(t) \rangle$ was substituted by the FACF obtained for $\tau_{\mathrm{v}0} = 0.1$ ps, $\left\langle \mathbf{F}^{\mathrm{sim}}(t; 0.1\ \mathrm{ps}) \cdot \mathbf{F}^{\mathrm{sim}}(0; 0.1\ \mathrm{ps}) \right\rangle$, which was found to approximate well the dynamics defined by Eqs. 16 and 17, as described in the following section. In these calculations, the numerical integration was performed using the trapezoidal formula.

4 | RESULTS AND DISCUSSION

4.1 | Smaller system

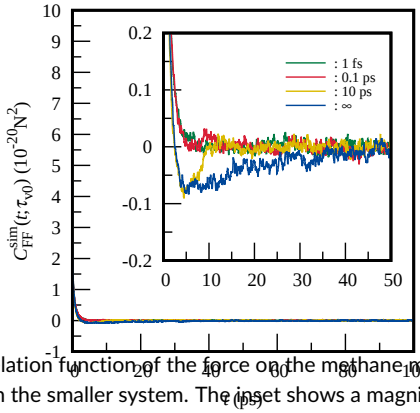

FIGURE 1 Time correlation function of the force on the methane molecule at $\tau_{\mathrm{v}0}$ = 1 fs (green), 0.1 ps (red), 10 ps (yellow), and ∞ (blue) in the smaller system. The inset shows a magnified view for $0 \leq t \leq 50$ ps.

Figure 1 shows time correlation functions of the force on the methane molecule at $\tau_{\mathrm{v}0}$ = 1 fs, 0.1 ps, 10 ps, and ∞ in the smaller system. This graph shows that the time correlation function for $\tau_{\mathrm{v}0} \leq 0.1$ ps converged to zero immediately. On the other hand, a negative correlation appears for $\tau_{\mathrm{v}0} \geq 10$ ps. Considering that the absence of the negative tail for the systems of $\tau_{\mathrm{v}0}$ = 1 fs and 0.1 ps can be ascribed to the fast decay of the tail, the larger $\tau_{\mathrm{v}0}$ is, the more slowly the negative correlation relaxes. The negative correlation for $\tau_{\mathrm{v}0} = 10$ ps disappears at approximately 10 ps. This means that the effect of the momentum given by the solute to the solvent disappears due to the shift in the COM velocity at times longer than $\tau_{\mathrm{v}0}$. The MB method calculates the diffusion coefficient by

$$D = \frac{3(k_{\mathrm{B}}T)^2}{\int_0^\infty \langle \Delta\mathbf{F}_X(0) \cdot \Delta\mathbf{F}_X(t) \rangle \, \mathrm{d}t}. \tag{23}$$

Here, Δ is appended to $\mathbf{F}_X(t)$ to describe explicitly the deviation from the mean force, however, Δ can be omitted in homogeneous systems as considered in this work. Equation 23 indicates that the diffusion coefficient is inversely proportional to the integrated value of FACF. Therefore, the fact that the shape of the time correlation function in Fig. 1 differs depending on $\tau_{\mathrm{v}0}$ means that the calculated diffusion coefficient also differs depending on $\tau_{\mathrm{v}0}$.

Figure 2 shows the running integrals of the time correlation functions of the force at $\tau_{\mathrm{v}0}$ = 1 fs, 0.1 ps, 10 ps,

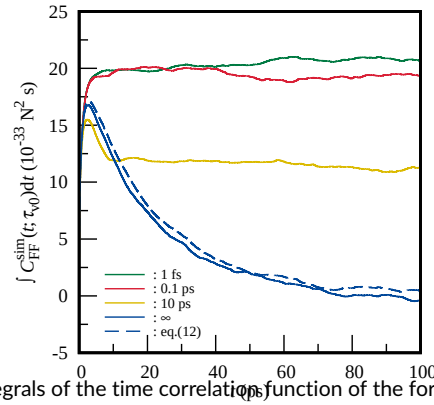

FIGURE 2 Running integrals of the time correlation function of the force on the methane molecule at τ_{v0} = 1 fs (green), 0.1 ps (red), 10 ps (yellow), and ∞ (blue) in the smaller system. The curve calculated by the right-hand side of Eq. 14 is shown by the blue dashed line.

and ∞ in the smaller system. When the time correlation function of the force converges to zero, the integrated value converges to a certain value. By substituting this converged value into Eq. 23, the diffusion coefficient can be estimated, and Fig. 2 clearly shows that the converged values differ depending on τ_{v0}. As mentioned in Section 2, the integral converges to the correct value when the COM velocity of the system is removed at every step. Therefore, the converged integral value at τ_{v0} = 1 fs is correct. For $\tau_{v0} \leq$ 0.1 ps, the running integral converged to the same value as that at τ_{v0} = 1 fs. This means that τ_{v0} = 0.1 ps would be sufficiently small to give accurate results for the size of the system in this MD calculation. As τ_{v0} increases, the converged value became smaller and smaller, and $\tau_{v0} = \infty$ converges to 0, which is consistent with Eq. 18. The physical explanation is that the momentum given by the solute to the solvent is finally returned to the solute, because $\tau_{v0} = \infty$ means the absence of a momentum sink other than the solute itself. Moreover, comparing the functional form of the calculation result until it converges to zero with the result from the theoretical equation (Eq. 14), the curve at $\tau_{v0} = \infty$ is consistent with the curve obtained from the theoretical equation. Therefore, the numerical calculations support the validity of our theory. The running integral at τ_{v0} = 10 ps follows the similar decay at $t < \tau_{v0}$, and converges to the finite value at the longer time. In other words, the theory elucidates that the diffusion coefficient from the MB method depends on the period (τ_{v0}) in which the COM velocity is removed during MD simulations. The theory thus captures the physical mechanism by which the choice of τ_{v0} affects the FACFs through the modification of the correlation functions.

4.2 | Larger system

Time correlation functions of the force on the methane molecule and their running integrals are shown in Figs. 3 and 4, respectively, at τ_{v0} = 0.1 ps, 10 ps, and ∞ in the larger system. Figure 3 shows that the negative correlation is weaker than that of the smaller system. As the MD system size increases, the momentum of the system is distributed over a larger space, and the COM velocity of the solvent generated by the momentum given by the solute becomes smaller. Therefore, the dependence on τ_{v0} becomes smaller as the system size of the MD calculations increases. For $\tau_{v0} = \infty$, the negative correlation is weaker than that in the smaller system, but its relaxation becomes slower, as

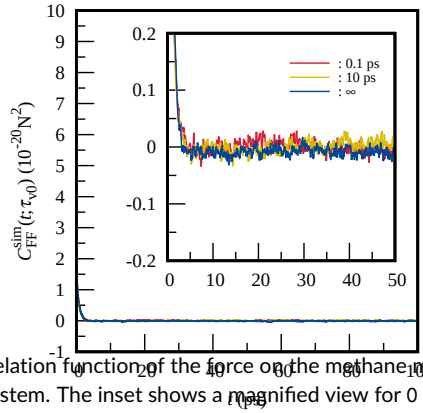

FIGURE 3 Time correlation function of the force on the methane molecule at τ_{v0} = 0.1 ps (red), 10 ps (yellow), and ∞ (blue) in the large system. The inset shows a magnified view for $0 \leq t \leq 50$ ps.

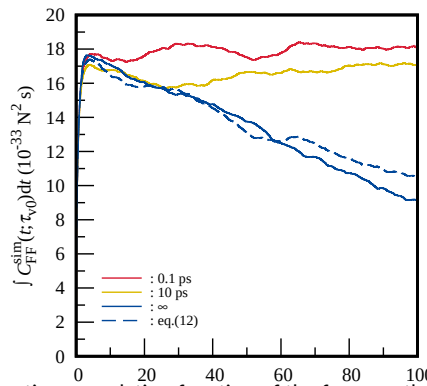

FIGURE 4 Integrating the time correlation function of the force on the methane molecule at τ_{v0} = 0.1 ps (red), 10 ps (yellow), and ∞ (blue) in the large system. The curve calculated by Eq. 14 is shown by the blue dotted line.

shown in Figure 4. Eq. 18 predicts theoretically that the running integral at $\tau_{v0} = \infty$ should converge to zero for any finite systems, but unlike the smaller system, here the convergence was not complete even at 100 ps. The reason for this slow relaxation is that the larger the system, the longer it takes for the momentum to return. The agreement between the MD simulation and the theoretical prediction of Eq. 14 is excellent, also in the larger system, Fig. 4, which further supports our theoretical discussion. Figure 4 shows that, for the larger system, the result with $\tau_{v0} = 10$ ps was close to the correct value ($\tau_{v0} = 0.1$ ps). Therefore, the larger the system size, the larger τ_{v0} can be set.

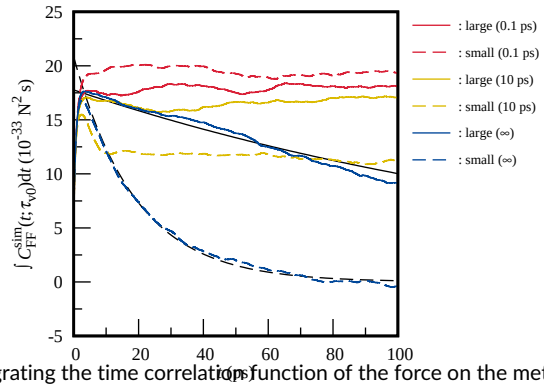

FIGURE 5 Integrating the time correlation function of the force on the methane molecule at $\tau_{v0} = 0.1$ ps (red), 10 ps (yellow), and ∞ (blue) in the large (solid line) and small (dashed line) systems. Eq. (19) of the large and small systems is shown by black solid and dashed lines.

According to Eq. 22, the τ_{FF} of the small and large systems were 19.1 and 174.7 ps, respectively. Eq. 21 is plotted using these τ_{FF} and regarding the amplitude as an adjustable parameter. In addition, the running integrals of the time correlation functions of the force on COM of the methane molecule in the larger and smaller systems are shown again in Fig. 5 to make their difference clearly visible. It can be seen that Eq. 20 reproduces the decay well at $\tau_{v0} = \infty$ for both the smaller and larger systems. τ_{FF} is a reference quantity for determining τ_{v0}, and the larger the τ_{FF}, the larger the value of τ_{v0} can be set. The larger the size of the system, the larger the value of τ_{FF}, which shows that τ_{v0} can be larger for larger systems. We mentioned in Section 4.2 that $\tau_{v0} = 0.1$ ps, which is one two-hundredths of τ_{FF}, is small enough to calculate D in the smaller system with sufficient accuracy. It is thus sufficient to set τ_{v0} to 1/200th of τ_{FF} even for a small system with fast decay. In the larger system, the result of $\tau_{v0} = 10$ ps, which is about 1/20th of τ_{FF} of the system, is close to that of $\tau_{v0} = 0.1$ ps. Therefore, it is safe to set τ_{v0} to at most 1/200th of τ_{FF} for any system larger than the smaller system.

For $\tau_{v0} \geq 10$ ps, the integral was larger for the larger system than that for the smaller one, indicating that the larger the size of the system, the longer the time part was affected, as discussed previously. However, at $\tau_{v0} = 0.1$ ps, the integral of the smaller system was larger than that of the larger system. This is not an effect of the shift of the COM velocity, but that of the hydrodynamic interaction between the solutes in adjacent cells in the periodic boundary system. Due to the effects of hydrodynamic interaction, the diffusion coefficient, D_{MD}, calculated from the MD calculation of the finite system with periodic boundary conditions, is shifted from the true diffusion coefficient

D_0 of the system of infinite size as shown in the following equation [36]:

$$D_{\mathrm{MD}} = D_0 - \frac{2.83729 k_{\mathrm{B}} T}{6\pi\mu L} \tag{24}$$

where μ and L are the viscosity coefficient and the length of the MD cell, respectively. This equation states that the smaller the cell size, the smaller D_{MD} becomes. Since the integral value of the time correlation function of the force is the reciprocal of D_{MD} (see Eq. 23), it becomes larger for smaller systems. Using the experimental viscosity coefficient of water at 25 °C ($\mu = 0.0009$ Pa·s) and Eq. 24, the difference in the integrated values of the time correlation functions of the force between the larger and the smaller systems was calculated to be 1×10^{-10} m$^2 \cdot$ s^{-1}. On the other hand, the difference found from our calculation, shown in Fig.5, is 2×10^{-10} m$^2 \cdot$ s^{-1}. So, the estimates from the theoretical equations of fluid mechanics and our calculation are in good agreement, considering the error guessed from the fluctuation of the running integral.

4.3 | Relevance to NVE ensemble and other thermostats

The formalized theory perfectly fits with the NVE ensemble, and thus the COM velocity shift is needed to eliminate the unwanted negative correlation between $\mathbf{F}(0)$ and $\mathbf{F}(t)$. However, the shift decreases the total energy when applied to the NVE simulations and therefore the simulations cannot reach thermal equilibrium. Furthermore, this decrease can cause a drop in the temperature and thus the diffusion constant can be underestimated. It should be carefully confirmed that the drift of the total energy or temperature is so marginal that the potential systematic error is satisfactorily small in application to NVE simulations. Given this potential artifact that is intrinsic to the NVE simulations, the coupling of a thermostat should be a practical choice, especially for long simulations, although disturbance from a thermostat to the original dynamics needs to be carefully considered. We have performed NVT simulations using a Nosé–Hoover thermostat in this work, and demonstrated that the discussion based on the NVE ensemble holds. We next discuss the applicability of the COM velocity shift to thermostats other than the Nosé–Hoover thermostat. Other widely used thermostats include the Gaussian constraint [37–40], velocity rescaling [41], and a Langevin thermostat [29].

A COM velocity shift is necessary for the thermostats that retain linear momentum conservation, such as the Gaussian constraint [37–40] and velocity rescaling [41], because the unwanted negative correlation between $\mathbf{F}(0)$ and $\mathbf{F}(t)$ arises ultimately from the momentum conservation (Eq. 7) in a finite system as described above. Furthermore, we have demonstrated numerically the necessity of the COM velocity shift for the Nosé–Hoover thermostat, which also retains the momentum conservation. When it comes to thermostats that break the momentum conservation, including the Langevin thermostat, we need to give more subtle consideration as follows.

When applying the Langevin thermostat, the coupling time constant τ_{LT} ($\tau_{\mathrm{LT}} \equiv 1/\gamma$, where γ is the damping coefficient of the thermostat) needs to be considered, as the thermostat works also as the momentum sink with this time constant τ_{LT}. If the coupling is sufficiently strong, i.e., $\tau_{\mathrm{LT}} \ll \tau_{\mathrm{FF}}$, the diminishing behavior of the running integral of $\langle \mathbf{F}_X(t) \cdot \mathbf{F}_X(0) \rangle$ should not be observed, because the COM momentum drops quickly. Nevertheless, because such a strong coupling might disturb the short-term dynamics as well, the potential artifact in the diffusion constant should be considered carefully. If the coupling is weak such that $\tau_{\mathrm{LT}} \gg \tau_{\mathrm{FF}}$, the running integral of $\langle \mathbf{F}_X(t) \cdot \mathbf{F}_X(0) \rangle$ should diminish, as the momentum drops too slowly. In this case, the COM velocity shift should be performed frequently enough such that $\tau_{\mathrm{v0}} \ll \tau_{\mathrm{FF}}$, even with this thermostat.

4.4 | Discussion on how to constrain the solute

4.4.1 | Harmonic constraint

The WR method is another popular method for evaluating the position-dependent diffusion coefficient [12]. In the WR method, the solute is constrained around a position of interest by a harmonic potential, and the spring constant of the potential, k, is an adjustable parameter. We hereafter discuss how the COM velocity shift of the solvent affects the diffusion coefficient when the solute is constrained to absolute coordinates in the WR method. For simplicity, we consider a homogeneous system where no potential of mean force is induced on the solute by the solvent. When the system size is infinite, the dynamics of the solute in the WR method is described by the generalized Langevin equation as

$$\dot{\mathbf{r}}_X(t) = \mathbf{v}_X(t), \tag{25}$$

$$m_X\dot{\mathbf{v}}_X(t) = \mathbf{F}_X(t), \tag{26}$$

$$\mathbf{F}_X(t) = \mathbf{R}_X(t) - \int_0^t d\tau\gamma(t-\tau)\mathbf{v}_X(\tau) - k\mathbf{r}_X(t). \tag{27}$$

Here, the mass, position, and velocity of the solute are denoted as m_X, $\mathbf{r}_X(t)$, and $\mathbf{v}_X(t)$, respectively, and the solute is assumed to be constrained to the origin. The equations above are solved to yield the time correlation function of the position as

$$\int_0^\infty dt\ \langle \mathbf{r}_X(0)\cdot\mathbf{r}_X(t)\rangle = \frac{\tilde{\gamma}_0}{k}\left\langle|\mathbf{r}_X(0)|^2\right\rangle, \tag{28}$$

$$\tilde{\gamma}_0 \equiv \int_0^\infty dt\gamma(t). \tag{29}$$

For derivation, readers refer to, e.g., Refs. 12,13,27,42 and also Sec. S2 of Supporting Information. Substituting the relationship between the fluctuation of the position and k as

$$\left\langle|\mathbf{r}_X(0)|^2\right\rangle = \frac{3k_BT}{k}, \tag{30}$$

the diffusion coefficient is determined by the equation as follows:

$$D = \frac{k_BT}{\tilde{\gamma}_0} = \frac{\left\langle|\mathbf{r}_X(0)|^2\right\rangle^2}{3\int_0^\infty dt\ \langle\mathbf{r}_X(0)\cdot\mathbf{r}_X(t)\rangle}. \tag{31}$$

We would like to note that Eq. 23 holds for finite k values [27] and that the diffusion constant obtained by Eq. 31 theoretically equals that obtained by Eq. 23.

Next we consider the finite-size system, to which the shift of the COM velocity of the solvent is applied with a time interval of τ_{v0}. Then, Eqs. 25 and 26 are intact, and Eq. 27 is modified as

$$\mathbf{F}_X(t) = \mathbf{R}_X(t) - \int_0^t d\tau\gamma(t-\tau)\left(\mathbf{v}_X(\tau) - \mathbf{v}_{CM}(\tau)\right) - k\mathbf{r}_X(t), \tag{32}$$

$$M_S\dot{\mathbf{v}}_{CM}(t) = -\left[\mathbf{F}_X(t) + k\mathbf{r}_X(t)\right] - \gamma_s M_S\mathbf{v}_{CM}(t). \tag{33}$$

Here, the shift of the COM velocity is approximated as the damping with a time constant of $\tau_{v0} = 1/\gamma_s$. The time

correlation function of the position is then obtained from Eqs. 25, 26, 32, and 33 as

$$\int_0^\infty dt\, \langle \mathbf{r}_X(0) \cdot \mathbf{r}_X(t) \rangle = \frac{\tilde{\gamma}_0}{k\left(1 + \frac{\tilde{\gamma}_0}{M_S \gamma_S}\right)} \left\langle |\mathbf{r}_X(0)|^2 \right\rangle, \tag{34}$$

whose derivation is described in Sec. S2 of Supporting Information. Comparing Eqs. 28 and 34, it is shown that the WR method gives the correct value of the diffusion coefficient under the condition as

$$\tau_{v0} = \frac{1}{\gamma_s} << \frac{M_S}{\tilde{\gamma}_0}, \tag{35}$$

which is the same condition as the MB method.

It is rather surprising that the condition Eq. 35 does not contain k. One may consider that τ_{v0} can be smaller with decreasing k, because the diffusion coefficient from the WR method reduces to that from the mean square displacement of the unconstrained solute, for which the shift of the COM velocity is unnecessary. However, Eq. 35 means that the removal of the COM velocity is indispensable in the WR method, irrespective of the strength of the constraining potential. The result above indicates that the COM velocity of the solvent should be removed with sufficient frequency when the solute is constrained to absolute coordinates, irrespective of how the constraint is performed.

4.4.2 | Constraint by relative coordinates

Instead of constraining to absolute coordinates, it is also common to constrain the relative coordinates of two substances in order to calculate the position-dependent diffusion coefficients in heterogeneous systems. For example, membrane permeation[43] or substrate adsorption[44] of small molecules, and the transport across a transmembrane channel of ions[45] are all discussed in terms of potential mean force (PMF) and the position-dependent relative diffusion coefficient between two substances such as a membrane and a molecule.

In this case, external forces do not work, and only internal forces do. Therefore, momentum does not flow toward the solvent, and the error discussed in this paper does not occur. Therefore, τ_{v0} can be determined solely by considering its original purpose to compensate the numerical errors in the Ewald calculation.

5 | CONCLUSION

It was shown theoretically that the position-dependent diffusion coefficient obtained using the MB method depends on τ_{v0}. For systems as small as 1000 molecules, the FACF integrals converge well at $\tau_{v0} \leq 0.1$ ps, indicating that the diffusion coefficient can be obtained with good accuracy. However, at $\tau_{v0} \geq 10$ ps, the integral converges to a value different from the correct one. The larger was τ_{v0}, the smaller the converged value of the FACF integral became. The converged value was zero at $\tau_{v0} = \infty$, which has good consistency with the theoretical prediction, thereby supporting the validity of our theory.

For a system as large as 8000 molecules, the converged value of the FACF integral was close to the correct one even when τ_{v0} was as large as 10 ps. In addition, the convergence of the integrated value became slower at $\tau_{v0} = \infty$. This result is also consistent with our theoretical prediction, and shows that our theory is applicable, irrespective of the system size. These calculations demonstrate the necessity of choosing τ_{v0} according to the size of the system when calculating the position-dependent diffusion coefficient by the MB method using MD calculation with the Ewald

method. From the point of view of the speed of MD calculation, removing the COM velocity of the system requires full communication between nodes of parallel computers, which slows down the calculation speed. Therefore, τ_{v0} is preferred to be as large as possible, but 0.1 ps is probably sufficient for ordinary systems.

Acknowledgments

TY was supported by a Grant-in-aid (KAKENHI) from Japan Society for the Promotion of Science (JSPS) (Grant No. 19K03768). KF was supported by KAKENHI from JSPS (Grant No. 20K05631) and MEXT as "Program for Promoting Researches on the Supercomputer Fugaku" (Environmentally benign functional chemicals: No. JPMXP1020200308). This work is also partially supported by the Nitto Foundation. We also thank the Research Center for Computational Science, Okazaki, Japan, for the use of its supercomputers.

Data Availability Statement

The data that support the findings of this study are available from the corresponding author upon reasonable request.

Supporting Information

Additional Supporting Information may be found in the online version of this article.

references

[1] Fujimoto, K., Fukai, M., Urano, R., Shinoda, W., Ishikawa, T., Omagari, K., Tanaka, Y., Nakagawa, A. and Okazaki, S., *Pure Appl. Chem.*, 2020, **92**(10), 1585–1594.

[2] Shinoda, W., *Biochim. Biophys. Acta, Biomembr.*, 2016, **1858**(10), 2254–2265.

[3] Awoonor-Williams, E. and Rowley, C. N., *Biochim. Biophys. Acta, Biomembr.*, 2016, **1858**(7), 1672–1687.

[4] Venable, R. M., Kr 辰 mer, A. and Pastor, R. W., *Chem. Rev.*, 2019, **119**(9), 5954–5997.

[5] Shen, M., Keten, S. and Lueptow, R. M., *J. Membr. Sci.*, 2016, **506**, 95–108.

[6] Surblys, D., Yamada, T., Thomsen, B., Kawakami, T., Shigemoto, I., Okabe, J., Ogawa, T., Kimura, M., Sugita, Y. and Yagi, K., *J. Membr. Sci.*, 2020, **596**, 117705.

[7] Kawakami, T. and Shigemoto, I., *Polymer*, 2014, **55**(24), 6309–6319.

[8] Kawakami, T., Shigemoto, I. and Matubayasi, N., *J. Chem. Phys.*, 2018, **148**(21), 214903.

[9] Takeuchi, K., Kuo, A.-T., Hirai, T., Miyajima, T., Urata, S., Terazono, S., Okazaki, S. and Shinoda, W., *J. Phys. Chem. C*, 2019, **123**(33), 20628–20638.

[10] Straub, J. E., Borkovec, M. and Berne, B. J., *J. Phys. Chem.*, 1987, **91**, 4995–4998.

[11] Marrink, S.-J. and Berensen, H. J. C., *J. Phys. Chem.*, 1994, **98**, 4155–4168.

[12] Woolf, T. B. and Roux, B., *J. Am. Chem. Soc.*, 1994, **116**(13), 5916–5926.

[13] Hummer, G., *New J. Phys.*, 2005, **7**(1), 34.

[14] Sicard, F., Koskin, V., Annibale, A. and Rosta, E., *J. Chem. Theory Comput.*, 2021, **17**(4), 2022–2033.

[15] Yang, S., Onuchic, J. N., Garc 鰐 a, A. E. and Levine, H., *J. Mol. Biol.*, 2007, **372**(3), 756–763.

[16] Hinczewski, M., Hansen, Y. v., Dzubiella, J. and Netz, R. R., *J. Chem. Phys.*, 2010, **132**(24), 245103.

[17] Schulz, R., Yamamoto, K., Klossek, A., Flesch, R., H 旦 nzke, S., Rancan, F., Vogt, A., Blume-Peytavi, U., Hedtrich, S., Sch 辰 fer-Korting, M., R 端 hl, E. and Netz, R. R., *Proc. Natl. Acad. Sci. U. S. A.*, 2017, **114**(14), 3631–3636.

[18] Comer, J., Chipot, C. and Gonz 叩 lez-Nilo, F. D., *J. Chem. Theory Comput.*, 2013, **9**(2), 876–882.

[19] T 端 rkcan, S., Alexandrou, A. and Masson, J.-B., *Biophys. J.*, 2012, **102**(10), 2288–2298.

[20] Nagai, T., Tsurumaki, S., Urano, R., Fujimoto, K., Shinoda, W. and Okazaki, S., *J. Chem. Theory Comput.*, 2020, **16**, 7239–7254.

[21] Liu, H.-S., Chen, K.-Y., Fang, C.-E. and Chiu, C.-c., *Electrochim. Acta*, 2021, **375**, 137915.

[22] Manrique, R., Wu, W. and Chang, J.-S., *J. Appl. Phycol.*, 2020, **32**(1), 291–297.

[23] Rivel, T., Ramseyer, C. and Yesylevskyy, S., *Sci. Rep.*, 2019, **9**(1), 5627.

[24] Yesylevskyy, S., Rivel, T. and Ramseyer, C., *Sci. Rep.*, 2019, **9**(1), 17214.

[25] Yang, H., Zhou, M., Li, H., Liu, L., Zhou, Y. and Long, X., *RSC Adv.*, 2019, **9**(67), 39046–39054.

[26] Manrique, R., Chang, J. and Wu, W., *IOP Conf. Ser.: Earth Environ. Sci.*, 2019, **268**(1), 012062.

[27] Daldrop, J. O., Kowalik, B. G. and Netz, R. R., *Phys. Rev. X*, 2017, **7**(4), 041065.

[28] Ewald, P. P., *Ann. Phys. (Berlin, Ger.)*, 1921, **369**(3), 253–287.

[29] Allen, M. P.; Tildesley, D. J., In Computer Simulation of Liquids;, OXFORD University Press, Great Clarendon Street, Oxford, OX2 6DP, United Kingdom, second ed., 2017.

[30] Balucani, U.; Zoppi, M., In Dynamics of the Liquid State;, Oxford University Press, Great Clarendon Street, Oxford, OX2 6DP, United Kingdom, 1994.

[31] Nosé, S., *Mol. Phys.*, 1984, **52**, 255–268.

[32] Hoover, W., *Phys. Rev. A*, 1985, **31**, 1695–1697.

[33] Abraham, M. J., Murtola, T., Schulz, R., Páall, S., Smith, J. C., Hess, B. and Lindah, E., *SoftwareX*, 2015, **1-2**, 19–25.

[34] Berendsen, H. J. C., Postma, J. P. M., van Gunsteren, W. F. and Hermans, J. In *Intermolecular Forces*, Pullman, B., Ed.; Springer, Dordrecht, Holland, 1981; pages 331–342.

[35] Jorgensen, W. L., Madura, J. D. and Swenson, C. J., *J. Am. Chem. Soc.*, 1984, **106**, 6638–6646.

[36] Yeh, I.-C. and Hummer, G., *J. Phys. Chem. B*, 2004, **108**(40), 15873–15879.

[37] Hoover, W. G., Ladd, A. J. and Moran, B., *Phys. Rev. Lett.*, 1982, **48**, 1818–1820.

[38] Evans, D. J., Hoover, W. G., Failor, B. H., Moran, B. and Ladd, A. J. C., *Phys. Rev. A*, 1983, **28**, 1016–1021.

[39] Zhang, F., *J. Chem. Phys.*, 1997, **106**, 6102–6106.

[40] Minary, P., Martyna, G. J. and Tuckerman, M. E., *J. Chem. Phys.*, 2003, **118**, 2510.

[41] Bussi, G., Donadio, D. and Parrinello, M., *J. Chem. Phys.*, 2007, **126**, 014101.

[42] Gaalswyk, K., Awoonor-Williams, E. and Rowley, C. N., *J. Chem. Theory Comput.*, 2016, **12**, 5609–5619.

[43] Lee, C. T., Comer, J., Herndon, C., Leung, N., Pavlova, A., Swift, R. V., Tung, C., Rowley, C. N., Amaro, R. E., Chipot, C., Wang, Y. and Gumbart, J. C., *J. Chem. Inf. Model.*, 2016, **56**(4), 721–733.

[44] Ren, K., Wang, Y.-P. and Liu, S., *Phys. Chem. Chem. Phys.*, 2020, **23**(2), 1092–1102.

[45] Ngo, V., Li, H., MacKerell, A. D., Allen, T. W., Roux, B. and Noskov, S., *J. Chem. Theory Comput.*, 2021, **17**(3), 1726–1741.

GRAPHICAL ABSTRACT

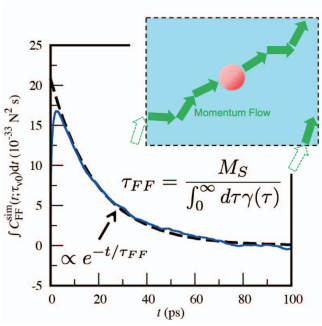

The position-dependent diffusion coefficient is beneficial for studying mass transport with molecular dynamics calculations. In the Marrink–Berendsen method, this coefficient can be obtained from the integral of force autocorrelation function of a fixed molecule at an absolute position. However, the integrated values evaluated so in a finite system diminishes due to momentum flows arising from momentum conservation, and the diffusion coefficient diverges unphysically. We rigorously demonstrate that frequent removals of total momentum eliminate this flaw.